IOP Publishing J. Phys. Mater. 5 (2022) 021002 https://doi.org/10.1088/2515-7639/ac4fa5

Journal of Physics: Materials

OPEN ACCESS

RECEIVED
5 November 2021

REVISED
15 December 2021

ACCEPTED FOR PUBLICATION
27 January 2022

PUBLISHED
10 February 2022

PERSPECTIVE

Perspective: multi-dimensional coherent spectroscopy of perovskite nanocrystals

Albert Liu[1,*], Diogo B Almeida[2], Lazaro A Padilha[2] and Steven T Cundiff[3]

[1] Max Planck Institute for the Structure and Dynamics of Matter, Hamburg, Germany
[2] Instituto de Física "Gleb Whataghin", Universidade Estadual de Campinas, Campinas, São Paulo, Brazil
[3] Department of Physics, University of Michigan, Ann Arbor, MI, United States of America
[*] Author to whom any correspondence should be addressed.

E-mail: albert.liu@mpsd.mpg.de

Keywords: multi-dimensional, coherent, spectroscopy, perovskites, nanocrystals

Supplementary material for this article is available online

Abstract

Recently, colloidal perovskite nanocrystals (PNCs) have emerged as an exciting material platform for optoelectronic applications due to their combination of facile synthesis routes, quantum size effects, and exceptional optical properties among other favorable characteristics. Given the focus on their optoelectronic properties, spectroscopic characterization of PNCs is crucial to rational design of their structure and device implementation. In this Perspective, we discuss how multi-dimensional coherent spectroscopy (MDCS) can resolve exciton dynamics and circumvent inhomogeneous broadening to reveal underlying homogeneous spectral lineshapes. We highlight recent applications of MDCS to PNCs in the literature, and suggest compelling problems concerning their microscopic physics to be addressed by MDCS in the future.

1. Introduction

The systematic synthesis and study of semiconductor nanocrystals spans four decades to early studies at the end of the 20th century [1–4]. Today the field continues to flourish, with new nanocrystal synthesis routes and architectures being discovered at a rapid pace. Among the most exciting recent developments is the synthesis of colloidal lead-halide perovskite nanocrystals (PNCs) [5], which have a perovskite lattice structure with an $APbX_3$ composition (where A is an organic or inorganic cation and X = Cl, Br, or I). PNCs combine the properties of colloidal nanocrystals, such as quantum size effects and versatile surface chemistry, with advantages inherited from their bulk counterparts. For example, the ionic bonding character [6] and defect-tolerant nature [7] of bulk lead-halide perovskites have translated to quantum efficiencies in PNCs nearing unity without the complication of shell over-coatings (necessary for comparable quantum efficiencies in traditional metal chalcogenide and pnictide nanocrystals [8]).

Despite their unique characteristics PNCs are not immune to many drawbacks of colloidal nanocrystals, most notably size and shape dispersion in ensembles. Because their exciton energy level structure is affected by quantum confinement, variation in nanocrystal geometry results in a concomitant variation of absorption and emission wavelength of electronic transitions. In such a situation optical lineshapes are broadened beyond the single-particle (homogeneous) linewidths, a phenomenon termed inhomogeneous spectral broadening. Inhomogeneous broadening is not only deleterious in many practical applications of PNCs, for example in lasing [9] and transport in superlattices [10], but also hampers study of their fundamental optoelectronic properties that manifest in homogeneous optical lineshapes.

To circumvent inhomogeneous broadening in spectroscopic studies of PNCs, single-nanocrystal spectroscopies are most commonly employed [11]. Such techniques isolate the homogeneous luminescence spectra of individual nanocrystals, albeit with significant drawbacks such as spectral diffusion and limited signal-to-noise ratio. Perhaps the most limiting aspect of single-nanocrystal spectroscopies however, is that lineshapes can vary dramatically between individual particles of an ensemble. A technique capable of resolving *ensemble-averaged* homogeneous lineshapes is multi-dimensional coherent spectroscopy (MDCS) [12], an optical analogue of nuclear magnetic resonance spectroscopy that has found applications in numerous disordered systems ranging from molecular liquids [13, 14] to atomic gases [15, 16], and even photosynthetic bacteria [17, 18].

The experimental implementations of MDCS and its application to semiconductor nanostructures have been previously discussed in dedicated reviews on these subjects [19–23]. However, it is only recently that MDCS has been applied to PNCs. The purpose of this Perspective is therefore to highlight some of the first studies on PNCs by MDCS in recent years and to outline some compelling questions that MDCS is uniquely poised to answer, with the hope of stimulating further activity in this burgeoning field.

2. Multi-dimensional coherent spectroscopy

Multi-dimensional coherent spectroscopy (MDCS) is a general class of nonlinear spectroscopic techniques that resolves a cross-section of, or even an entire, (complex-valued) nonlinear optical response $S^{(n)}$ of order n. Below, we describe some experimental implementations of MDCS and two common types of multi-dimensional spectra that are useful in the context of colloidal nanocrystals.

2.1. Experimental implementation

In general, measurement of a system's optical response function requires excitation by light. Measurement of a frequency-domain response function may be accomplished by excitation with continuous-wave light sources of variable frequency or by excitation with pulsed light sources of variable time-delays. Fourier transform spectroscopy methods with pulsed excitation are far more commonplace, which are therefore assumed below.

There are two general requirements for experimental implementations of MDCS. First, inter-pulse time-delays that involve coherence evolution must be stable to within a fraction of the excitation light period. Second, a nonlinear optical response must be separated from the linear optical response, which is stronger at low excitation fluences. This second requirement may be accomplished in either a non-collinear excitation geometry by wave-vector phase-matching (see supplemental information available online at stacks.iop.org/JPMATER/5/021002/mmedia) [24] or in a collinear excitation geometry by phase-cycling [20].

Most commonly, MDCS measures a third-order optical response $S^{(3)}$ by using three excitation fields to generate a four-wave mixing signal. The dynamics induced by each excitation pulse are usually interpreted in a perturbative framework, in which each field interaction induces a change in a system's density matrix. These changes altogether constitute so-called quantum pathways, which provide a physical interpretation of the peaks observed in multi-dimensional spectra. As illustrated in figure 1(a), the first pulse (A) generates a coherent superposition between the ground and an optically active excited state, which oscillates at the transition energy $\hbar\omega_\tau$. The second pulse (B) then converts this interband coherence into either a population state that decays according to its relaxation rate or an intraband coherence between two neighboring states within a ground or excited state manifold [25] that oscillates at the intraband energy splitting $\hbar\omega_T$. The last pulse (C) then generates a final interband coherence that oscillates at its respective transition energy $\hbar\omega_t$ and radiates an FWM signal. We leave further description of the analytical expressions to other more detailed texts [26].

If the phase-stability criteria introduced above is satisfied, the time-domain four-wave mixing signal may be measured and Fourier transformed along two or more time axes to generate a multi-dimensional spectrum. Although many different multi-dimensional spectra are possible depending on both the chosen pair of time axes and the pulse time-ordering, we describe below two types of spectra that have proven particularly useful in the study of PNCs, termed one-quantum and zero-quantum spectra. A model system comprised of two coupled inhomogeneously broadened transitions, one of resonance energy $\hbar\omega_1$ and another of resonance energy $\hbar\omega_2$ (shown in figure 1(b)), is simulated to demonstrate the basic features in multi-dimensional spectra of disordered level systems.

2.2. One-quantum spectra

One-quantum spectra are obtained by Fourier transform along the time-delays $\{\tau, t\}$. Interband coherence evolution occurs along these two delays, as represented by the high-frequency oscillations in figure 1(a), and therefore one-quantum spectra correlate absorption and emission dynamics of a given material system. In the case of rephasing one-quantum spectra [19, 23], coherences evolve with inverse phase between delays τ and t (reflected in negative absorption energy $\hbar\omega_\tau$), which is assumed henceforth. A schematic one-quantum spectrum (simulated for the model system in figure 1(b)) is shown in figure 1(c), which illustrates two unique capabilities:

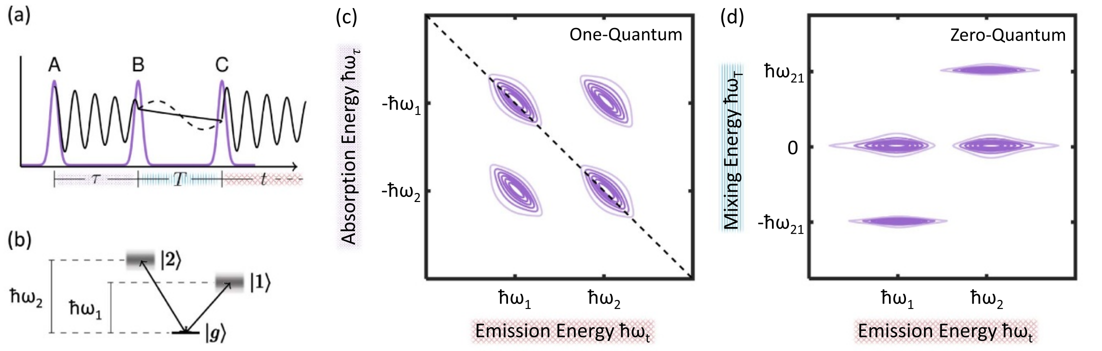

Figure 1. (a) Generic pulse sequence used in MDCS measurements to generate a nonlinear optical signal. In the case of four-wave mixing, the dynamics induced by each pulse may be interpreted perturbatively, in which pulses A and C generate interband coherences that oscillate at the transition resonance energy, while pulse *B* can either generate a population state that undergoes relaxation or an intraband coherence that oscillates at the energy difference between two states of a manifold. (b) Model system simulated in ((c), (d)) that is comprised of two transitions of resonance energy $\hbar\omega_1$ and $\hbar\omega_2$, both of which are inhomogeneously broadened. (c) One-quantum and (d) zero-quantum spectra simulated for the model system in (b), in which the axes are highlighted according to their respective Fourier conjugate axis in (a).

- Two peaks are present at $|\hbar\omega_\tau| = |\hbar\omega_t|$ (indicated by the dashed black line), which correspond to absorption and emission involving identical photon energies. Two additional peaks are present at $|\hbar\omega_\tau| \neq |\hbar\omega_t|$, which then correspond to absorption and emission involving different photon energies. One-quantum spectra therefore reveal coupling between different optical transitions through the presence of the latter so-called cross-peaks.
- The peaks are elongated along the $|\hbar\omega_\tau| = |\hbar\omega_t|$ direction, which illustrates the presence of two distinct broadening mechanisms. Namely, homogeneous broadening due to the single-particle oscillator damping and inhomogeneous broadening due to disorder (see figure 1(b)) are projected in orthogonal directions in a one-quantum spectrum [27]. In contrast, a homogeneously-broadened resonance (absent of disorder) would manifest as a completely symmetric peak along both axes. It should also be noted that, unlike the homogeneous lineshapes measured by single-nanocrystal photoluminescence, the lineshapes measured by MDCS for time-delay $T \approx 0$ reflect the exciton transition in the absence of population dynamics (such as Stokes shift and spectral diffusion) following optical absorption.

We remark that a one-quantum spectrum, which plots the optical response cross-section $S^{(3)}(\omega_t, T, \omega_\tau)$, may be viewed as a generalized pump-probe response that resolves both quadratures of the complex optical response with pump spectral resolution limited only by Fourier transform parameters. For example, a transient absorption measurement is expressed in terms of the optical response function as [28, 29]:

$$\Delta A(\omega_t, T) \approx \mathrm{Re} \int_{-\infty}^{\infty} E_{\mathrm{pump}}(\omega_\tau) S^{(3)}(\omega_t, T, \omega_\tau) d\omega_\tau, \tag{1}$$

where the only approximation is that of an infinitely broad probe pulse spectrum (which approximates the usual case of a white-light continuum probe pulse). An equivalent transient absorption spectrum may therefore be extracted from a one-quantum spectrum by windowing the optical response along the vertical absorption axis by the excitation spectrum E_{pump} and subsequent projection onto the horizontal emission axis.

2.3. Zero-quantum spectra

Zero-quantum spectra are obtained by Fourier transform along the time-delays $\{T, t\}$. Both population relaxation and intraband coherence evolution occurs along the delay T, as represented by the solid and dashed curves in figure 1(a), and therefore zero-quantum spectra correlate these dynamics with subsequent optical emission along the delay t. A zero-quantum spectrum (simulated for the same model system in figure 1(b)) is shown in figure 1(d), which illustrates how population dynamics and intraband coherences manifest in frequency space.

- Population relaxation manifests as peaks at zero mixing energy ($\hbar\omega_T = 0$). The widths of each peak along the horizontal emission energy direction reflect the resonance energy distribution of each respective resonance, while the widths along the vertical mixing energy direction reflect their population relaxation times.

- Intraband coherence evolution manifests as peaks at non-zero mixing energy ($\hbar\omega_T \neq 0$), specifically at the energy splitting between the two states involved. The width along the vertical mixing energy direction reflects the intraband coherence dephasing time while tilt of a sideband (in the inhomogeneously broadened case) may reveal dispersion of an intraband energy splitting.

We note that the spectrum in figure 1(d) is simulated for perfectly correlated inhomogeneity between the two transitions (a good assumption for most nanocrystal systems). If this is not the case, vertical mixing energy width then gains a contribution from disorder of the intraband energy splitting $\hbar\omega_{12}$.

2.4. MDCS of colloidal nanocrystals

MDCS of colloidal nanocrystals may, at the most basic level, be understood in terms of dipole transitions between discrete energy levels arising from three-dimensional quantum confinement. While this suggests a close correspondence between electronic excitations in molecular systems and excitons in colloidal nanocrystals, the physics revealed in multi-dimensional spectra suggest a more nuanced description.

Indeed, much of the physics of colloidal nanocrystals is inherited from their bulk parent compounds. Acoustic [30] and optical phonon modes [31] of a crystal lattice couple to excitons in nanocrystals, just as in bulk semiconductors. Especially for colloidal nanocrystals of extended dimensions such as nanoplatelets, many-body effects can also play a primary role in their optical properties [32].

It should be emphasized however, that most of the new physics introduced in colloidal nanocrystals possess direct analogues in the physics of molecular systems. For example, the limited size of nanocrystals gives rise to discrete vibrational modes confined to their geometry [33], reminiscent of molecular bond vibrations. Excitons in nanocrystals also experience a fluctuating energetic environment as in molecular liquids, whether due to solvation dynamics [34] or charge migration [11]. Multi-dimensional spectra of colloidal nanocrystals may therefore be understood using intuition borrowed from the physics of both bulk semiconductors and molecules.

2.5. Limitations of MDCS

We conclude this section by discussing possible limitations of MDCS compared to conventional linear spectroscopies.

- To perform linear spectroscopies only a single excitation light source and direct, incoherent signal measurement by a photodetector is required. Experimental realization of MDCS is more complex, as two/three excitation pulses must be guided to the sample with variable, phase-stable time-delays, and the generated nonlinear optical signal is then combined with a separate local-oscillator pulse for phase-sensitive detection.
- Excitation fields that are sufficiently high to generate a nonlinear optical response are required, which may near damage thresholds for certain materials.
- The spectral content of each excitation pulse determines possible features in resultant multi-dimensional spectra. Sufficient spectral bandwidth is therefore required for broad peak linewidths or large energy separations between resonances.

3. Interband dynamics

Interband dynamics play a primary role in optoelectronic applications of PNCs, which encompass optical absorption/emission as well as charge/energy transfer following photoexcitation. As discussed in the previous section, one-quantum spectra probe these dynamics by correlating the photon energy of initial optical absorption with the photon energy of subsequent optical emission. In this section we discuss some representative studies of interband dynamics in PNCs using MDCS.

3.1. Exciton homogeneous linewidth

In one-quantum spectra, homogeneous and inhomogeneous resonance lineshapes are projected in orthogonal directions [27]. MDCS is therefore capable of extracting the ensemble-averaged homogeneous linewidth of exciton resonances in PNCs, even in the presence of strong inhomogeneous broadening. To this end, Liu *et al* recently applied MDCS to $CsPbI_3$ nanoplatelets at cryogenic temperatures [32]. As shown in figure 2, one-quantum spectra of 2-layer and 3-layer nanoplatelets exhibit Lorentzian homogeneous lineshapes reflecting Markovian (memory-less) exponential dephasing with dramatically different homogeneous and inhomogeneous linewidths. Extrapolating the homogeneous linewidth to room-temperature, these measurements [32] suggested that thin (2-layer) nanoplatelets were homogeneously-broadened at room-temperature while increasing out-of-plane thickness violates this

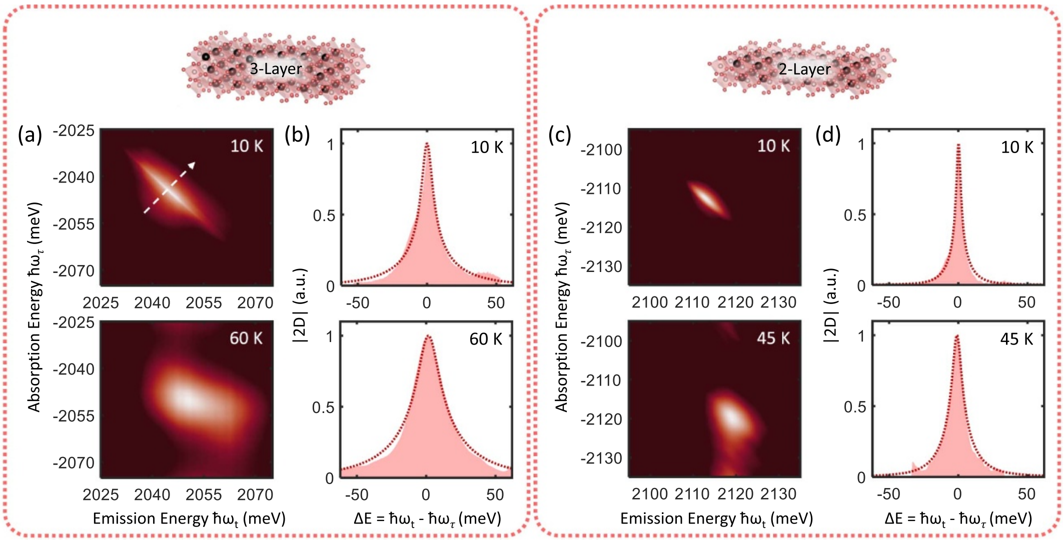

Figure 2. ((a), (c)) Magnitude one-quantum spectra of (a) three-layer and (c) two-layer $CsPbI_3$ nanoplatelets in glass at the indicated temperatures. ((b), (d)) Cross-diagonal slices of the (b) three-layer and (d) two-layer one-quantum spectra centered at 2045 and 2113 meV, respectively. The cross-diagonal slice location for the 10 K slice in (b) is indicated by the white dashed arrow in (a). Experimental data and line shape fits (for Lorentzian lineshapes corresponding to exponential dephasing) are plotted as the shaded area plots and dotted lines, respectively. Apdated with permission from [32]. Copyright (2021) American Chemical Society.

common assumption in nanoplatelets [35, 36]. In addition to elucidating homogeneous broadening mechanisms via temperature- and excitation fluence-dependent measurements, the homogeneous linewidth was further resolved as a function of exciton resonance energy to inform the effect of variations in nanoplatelet geometry. Such an analysis provides a unique view into the effects of quantum confinement on excitons in PNCs, a contentious topic in itself [37].

Similar measurements have also been performed by Yu *et al* [38] on $CsPbBr_3$ nanocubes, which revealed exciton-phonon coupling to acoustic vibrational modes to be the dominant homogeneous line-broadening mechanism. This conclusion is similar to what was found for $CsPbI_3$ nanoplatelets [32]. In contrast, increasing excitation fluence was found to have a minimal effect on the measured homogeneous linewidth, which is not the case for $CsPbI_3$ nanoplatelets [32], highlighting the importance of nanocrystal dimensionality on exciton-exciton scattering in PNCs.

3.2. Exciton fine-structure

Exciton fine-structure states in PNCs share a common ground state, and therefore lead to cross-peaks in one-quantum spectra. For inhomogeneously-broadened ensembles, these cross-peaks are elongated into sidebands that inform the fine-structure energy splittings and dephasing rates.

An interesting aspect of the exciton fine-structure of PNCs lies in their orthogonal linear transition dipole moments, which allow for polarization-selective excitation of individual states in the triplet manifold. Thus far, polarized fine-structure emission has primarily been observed in single-nanocrystal spectroscopies [39, 40], which suffer from limited signal-to-noise ratio and variation between individual nanocrystals. With polarization-resolved MDCS however, the fine-structure selection rules are preserved in ensemble measurements even in the presence of nanocrystal orientation disorder [41]. Such an experiment was recently performed by Liu *et al* on $CsPbI_3$ nanocubes, in which one-quantum spectra were acquired with two different excitation polarization schemes termed co-linear and cross-linear (shown in figure 3(a)). In the spectra shown in figure 3(b), dramatically different lineshapes are observed between the two polarization schemes due to enhancement and suppression of different fine-structure transitions. The polarization-dependent lineshapes were then used to fit dephasing times between the different triplet state transitions and to infer a partially-bright triplet exciton band-edge [42].

We finally mention that exciton fine-structure may also manifest in one-quantum spectra as coherent dynamics during the time-delay T. In exemplary measurements of $MAPbBr_3$ nanocrystals in a strongly quantum-confined size regime, Wang *et al* reported coherent oscillations of one-quantum spectra with varying delay T [43]. Though the nature of these oscillations could not be ascertained as vibronic or purely electronic, low-temperature measurements were proposed as a potential route to resolve this ambiguity.

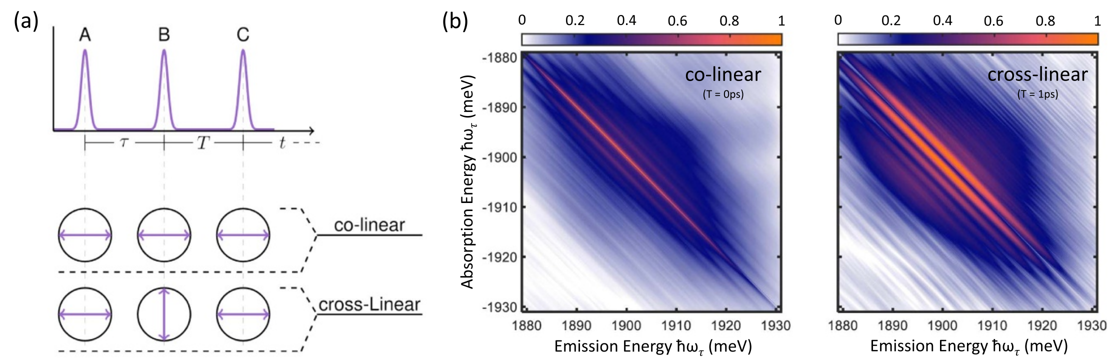

Figure 3. (a) Excitation pulse sequence and excitation polarization schemes in which double-sided arrows in circles denote the polarization of each pulse. Pulses A and C are horizontally polarized, and pulse B is either horizontally or vertically polarized, which corresponds to an emitted signal of either horizontal or vertical polarization respectively. (b) Magnitude one-quantum spectra of $CsPbI_3$ nanocrystals in glass at 4.6 K with co-linear and cross-linear excitation respectively. From [42]. Adapted with permission from AAAS.

3.3. Exciton–phonon coupling

In both PNCs and nanocrystals more broadly, exciton-phonon coupling constitutes a primary mechanism of coherence dephasing [44] and energy transfer [45]. From a spectroscopic perspective exciton-phonon coupling manifests in two primary ways, namely in homogeneous spectral lineshapes and oscillatory dynamics due to coherent nuclear motion [46].

To be more precise, homogeneous lineshapes of exciton resonances are comprised of three components: (1) zero-phonon lines representing an exciton resonance without phonon involvement [44, 45], (2) non-Lorentzian phonon pedestals due to inelastic scattering with phonons spanning a continuous range of eigenenergies (i.e. acoustic vibrations) [30], and (3) phonon sidebands (replicas) due to inelastic scattering with phonons of discrete eigenenergies (i.e. optical or quantum-confined vibrations) [47]. Broadening of the zero-phonon line with temperature then informs elastic scattering with phonons of both discrete and continuum eigenenergies. Indeed, recent publications by Yu *et al* [38] and Liu *et al* [32] have reported zero-phonon line broadening dominated by acoustic-phonon scattering in $CsPbBr_3$ nanocubes and $CsPbI_3$ nanoplatelets respectively. While no clear signatures of acoustic phonon pedestals or sidebands were observed in the nanoplatelet spectra [32], more complex lineshapes are evident in the one-quantum spectra of both $CsPbBr_3$ [38] and $CsPbI_3$ [42] nanocubes that indicate inelastic scattering channels involving many vibrational modes. Dimensionality thus plays a primary role in determining exciton-phonon coupling in PNCs [48].

Complementary information may also be obtained by MDCS about the electronic dynamics that arise from exciton-phonon coupling. During the intermediate time-delay T, exciton-phonon coupling can give rise to coherent oscillations at characteristic vibrational frequencies. These oscillations may be thought of as vibrational coherences on either a ground or an excited electronic potential energy surface, with their own vibronic dephasing times. Recently Zhao *et al* reported T-dependent one-quantum spectra of $CsPbBr_3$ nanocubes, in which coherent oscillations were observed of the exciton resonance at room temperature [49]. As shown in figure 4, vibrational coherences on the ground and excited electronic potential energy surfaces were separated in frequency space according to their ground-state bleach and stimulated-emission quantum pathways respectively. We emphasize that this separation of ground and excited state coherences would not be possible via other techniques such as transient absorption spectroscopy [50], and requires the full complex-valued optical response.

3.4. Excited-state dynamics

The dynamics that evolve along the T time-delay also include incoherent processes such as spectral diffusion and population relaxation. Spectral diffusion dynamics, which refer to resonance energy fluctuations in time [11], are of particular interest on the ultrafast timescale as a microscopic origin of coherence dephasing [31] and spectral line-broadening. In an interesting report from Seiler *et al* [51] the spectral dynamics of $CsPbI_3$ nanocrystals were resolved as a function of T and compared with those of conventional CdSe nanocrystals and a molecular dye (shown in figure 5). Broadening of the homogeneous linewidth with increasing T, a direct measure of spectral diffusion [52, 53], was then used to quantify the polaronic dynamics in PNCs. While the diffusive dynamics were dissimilar to those of covalently-bonded CdSe nanocrystals, in which the homogeneous linewidth was coherently modulated at the LO-phonon frequency, they were reminiscent of

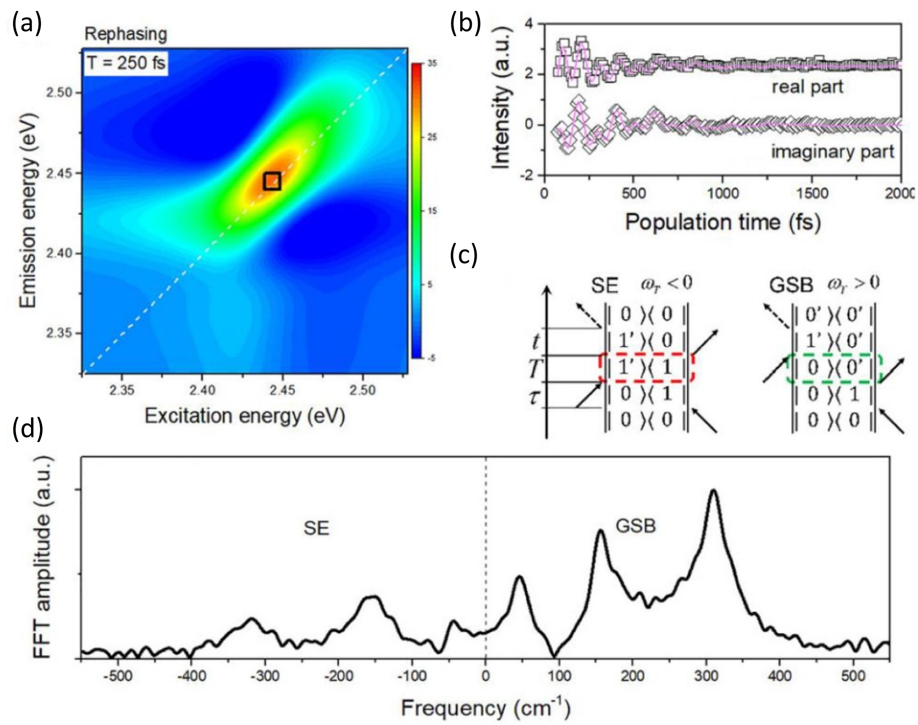

Figure 4. (a) Real-quadrature one-quantum spectrum of a solution sample of $CsPbBr_3$ nanocrystals. (b) Real and imaginary quadratures of the complex-valued one-quantum spectra as a function of T at the position indicated by the black square in (a). (c) Feynman diagrams representing stimulated-emission (SE) and ground-state bleach (GSB) quantum pathways that lead to vibronic oscillatory dynamics. The intermediate components of the SE and GSB Feynman diagrams that evolve during T, indicated by the dashed red and green boxes respectively, correspond to negative and positive evolution frequencies. (d) Fourier transform of the complex oscillations shown in (b) which separates the SE and GSB quantum pathways in the negative and positive frequency quadrants respectively. Adapted from [49], with the permission of AIP Publishing.

spectral diffusion in the molecular dye Nile Blue. Time-resolved measurements of the homogeneous linewidth enabled by MDCS thus provide an interesting conceptual analogy between polaron formation and solvation dynamics.

Beyond spectral diffusion dynamics, dynamically-varying spectral weight of peaks in one-quantum spectra may be ascribed to incoherent charge or energy transfer between resonances. In a recent report by Yu *et al* the incoherent relaxation dynamics of hot carriers to the band-edge exciton state were measured in this way with femtosecond ($<$10 fs) time-resolution [54]. Relaxation times were measured for a range of nanocrystal sizes, through which phonon-bottlenecking [55] was directly inferred with increasing quantum confinement. Crucial to this observation was also the combination of high temporal and energy resolution possible in Fourier transform spectroscopies such as MDCS. In contrast, conventional pump-probe techniques such as transient absorption spectroscopy suffer from a trade-off between temporal and energy resolution due to the Fourier transform limit of excitation pulses.

4. Intraband dynamics

In the previous section, we have described how one-quantum spectra exhibit both coherent and incoherent dynamics along the time-delay T. If these dynamics are of particular interest, it is often advantageous to acquire zero-quantum spectra (rather than a full three-dimensional dataset) to correlate the dynamics during T with the subsequent optical emission. In this section we focus specifically on studies of intraband coherences in PNCs using MDCS, which can be of either vibrational or electronic origin.

4.1. Vibrational intraband coherences

It is shown in figure 4 that electron-phonon coupling involving vibrations of discrete energy may give rise to coherent oscillations along T, a form of vibrational intraband coherence. In zero-quantum spectra, these oscillations manifest as sidebands that correlate the vibronic energy and lifetime with the exciton emission energy. In figure 6(a), a zero-quantum spectra of $CsPbI_3$ nanocrystals is shown for co-linear excitation, in which three sidebands are observed at mixing energies $\hbar\omega_T = -3.3$, -5.5, and -14.9 meV due to coupling to three distinct vibrational modes. We note that the asymmetry of these sidebands, referring to a lack of

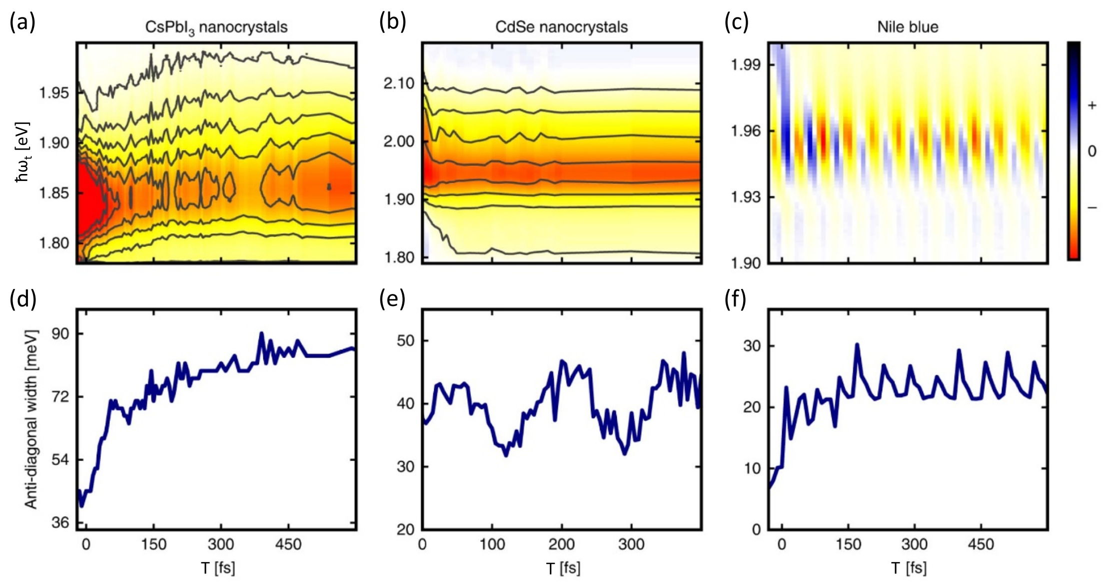

Figure 5. (a)–(c) Slices obtained for a given absorption energy $\hbar\omega_\tau$ in one-quantum spectra as a function of emission energy $\hbar\omega_t$, which may be considered pseudo-transient absorption spectra. The (a) $CsPbI_3$ spectra are shown for $\hbar\omega_\tau = 1.82$ eV. The (b) CdSe and (c) Nile Blue pseudo-TA maps are both shown for E1 = 1.95 eV. ((d)–(f)) Extracted cross-diagonal linewidths from the 2D spectra shown as a function of T for (d) $CsPbI_3$, (e) CdSe, (f) and Nile Blue as indicated. Adapted from [51]. CC BY 4.0.

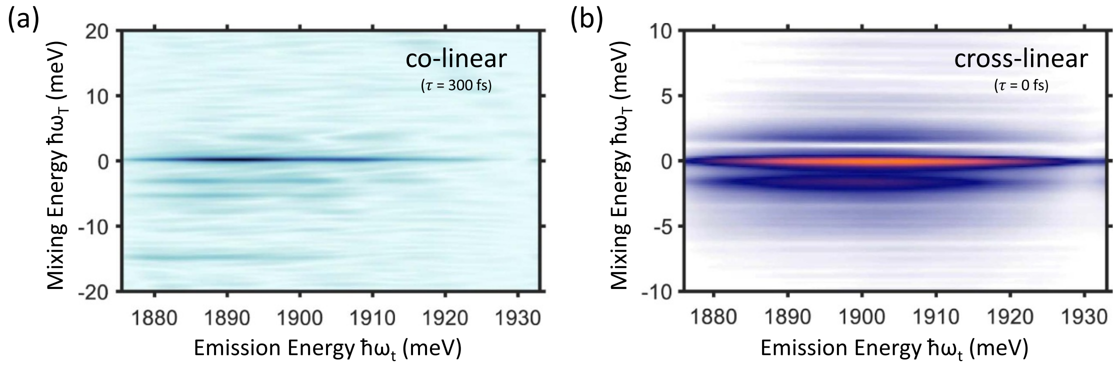

Figure 6. Magnitude zero-quantum spectra of $CsPbI_3$ nanocrystals in glass at 20 K with (a) co-linear and (b) cross-linear excitation respectively. From [42]. Adapted with permission from AAAS.

sidebands at positive mixing energy, is a signature of their vibrational nature [31, 46, 56]. Intraband coherences of purely electronic origin would instead exhibit symmetric sidebands of both oscillation polarities, which is discussed below.

4.2. Electronic intraband coherences

In PNCs, structural phase transitions away from the high-temperature cubic phase lift the degeneracy of the triplet exciton states [57]. Superpositions of these non-degenerate fine-structure states, a form of electronic intraband coherence, is of primary importance for many quantum coherent applications of PNCs such as single-photon emission [58]. In figure 6(b), a zero-quantum spectra of the same $CsPbI_3$ nanocrystals is shown for cross-linear excitation, in which symmetric sidebands at ± 1.6 meV are observed that arise from intraband coherences between two non-degenerate triplet exciton states. By measuring zero-quantum spectra as a function of temperature and fitting the resultant lineshapes, Liu *et al* showed that these intraband triplet coherences exhibit both a long coherence time of 1.36 ps (at a temperature of 20 K) and minimal thermal dephasing [42]. These properties compare favorably to those of candidate materials [59] for valleytronic applications [60], thus suggesting PNCs as a potential material platform for quantum information processing.

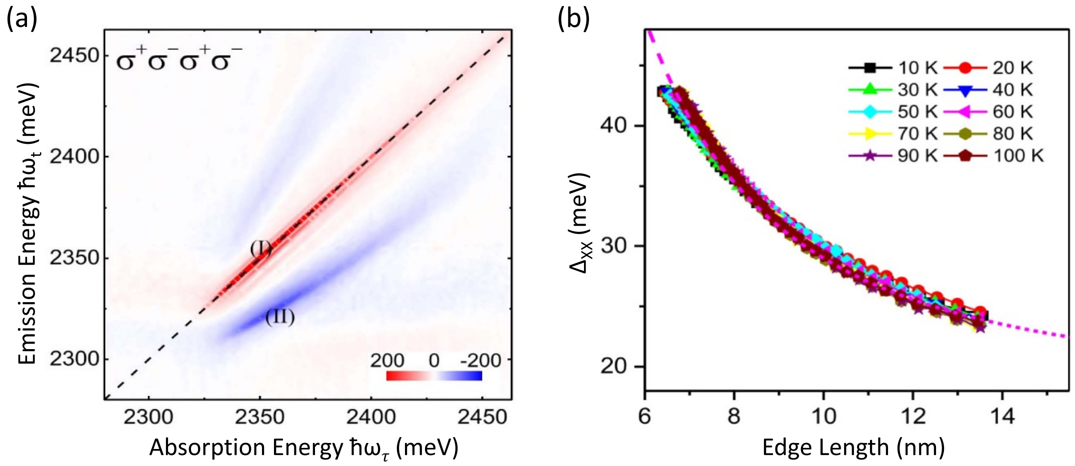

Figure 7. (a) Real-quadrature one-quantum spectrum of a film sample of $CsPbBr_3$ nanocrystals acquired with a cross-circular ($\sigma^+\sigma^-\sigma^+\sigma^-$) polarization scheme. A positive-valued single-exciton peak (labeled (I) is observed along the diagonal line ($|\hbar\omega_\tau| = |\hbar\omega_t|$) and a negative-valued biexciton peak (labeled II) is observed at an emission energy red-shifted by the biexciton binding energy. (b) Extracted biexciton binding energy as a function of nanocrystal edge length, which exhibits a characteristic $1/r^2$ dependence. Adapted with permission from [61]. Copyright (2020) American Chemical Society.

5. Higher-order exciton complexes

In third-order MDCS that measures a four-wave mixing signal, certain quantum pathways termed excited-state absorption involve emission from doubly-excited states. Biexciton resonances in PNCs thus manifest in one-quantum spectra, specifically as negative peaks in the real-quadrature component [62]. This was observed in a recent study by Huang *et al* which applied MDCS to $CsPbBr_3$ PNCs in order to extract the biexciton binding energy as a function of nanocrystal size and temperature [61]. As shown in the real-quadrature one-quantum spectrum plotted in figure 7(a), a negative peak is observed that is red-shifted along the emission energy axis (relative to the positive single-exciton peak located at $|\hbar\omega_\tau| = |\hbar\omega_t|$) by a value identical to the biexciton binding energy. This binding energy is plotted in figure 7(b) as a function of nanocrystal size, which exhibits a characteristic $1/r^2$ dependence that is largely independent of temperature. Finally, we note a related study by Zhao *et al* that revealed the mechanisms of optical gain in $CsPbBr_3$ PNCs [49].

6. Final remarks

We have performed a brief overview of multi-dimensional spectroscopy (MDCS), and surveyed the literature thus far applying MDCS to PNCs. Even as a burgeoning field, MDCS of PNCs has provided unique insights into their microscopic physics such as intrinsic linewidths, triplet exciton fine-structure, polaron formation, and biexciton resonances. However, these studies give merely a glimpse into the potential breadth of physics in PNCs to be explored by this technique.

From our point of view, among the most interesting physics reveal themselves at cryogenic temperatures. For example, population transfer between the triplet exciton states as well as between the neighboring dark singlet state may be resolved in time using MDCS. At sufficiently low temperatures the coherence dephasing dynamics also become non-Markovian, resulting in spectral lineshapes that reflect the spectral density of exciton-acoustic phonon coupling [30].

Another interesting direction is in terms of action-based MDCS techniques that detect signals other than coherent optical emission. For example, photoluminescence-detected MDCS [63] isolates the quantum pathways leading to incoherent luminescence and can inform the mechanisms that limit the performance of light-emitting devices. Photocurrent-detected MDCS [64] could also address many interesting questions concerning transport and other collective phenomena in PNC superlattices [10, 65].

Lastly, the unique insight into multiple-exciton dynamics afforded by MDCS yields a rich area of investigation. Biexciton fine-structure, and even higher-order exciton species such as triexcitons may be directly characterized by MDCS [66]. The addition of an incoherent pre-pulse prior to each MDCS measurement also introduces a host of new multiple-exciton phenomena that manifest in multi-dimensional spectra. For example, a high-photon energy pre-pulse could excite hot-carriers which undergo impact ionization to generate multiple excitons. Varying a time-delay between this pre-pulse and a subsequent MDCS measurement would then constitute a direct measurement of carrier multiplication in PNCs [67].

Data availability statement

No new data were created or analysed in this study.

Acknowledgment

Albert Liu was supported by a fellowship from the Alexander von Humboldt Foundation. D B A acknowledges the support from São Paulo Research Foundation (FAPESP), under Grant No. 2019/22576-8. D B A and L A P acknowledge the funding from FAPESP (Grant No. 2108/15574-6).

ORCID iDs

Albert Liu https://orcid.org/0000-0001-6718-3719
Diogo B Almeida https://orcid.org/0000-0003-2369-4618
Lazaro A Padilha https://orcid.org/0000-0002-8825-6611
Steven T Cundiff https://orcid.org/0000-0002-7119-5197

References

[1] Efros A L and Efros A L 1982 Interband light absorption in semiconductor spheres *Sov. phys. Semiconduct.* **16** 772
[2] Rossetti R, Ellison J L, Gibson J M and Brus L E 1984 Size effects in the excited electronic states of small colloidal cds crystallites *J. Chem. Phys.* **80** 4464
[3] Ekimov A I, Efros A and Onushchenko A A 1985 Quantum size effect in semiconductor microcrystals *Solid State Commun.* **56** 921
[4] Brus L 1986 Electronic wave functions in semiconductor clusters: experiment and theory *J. Phys. Chem.* **90** 2555
[5] Protesescu L, Yakunin S, Bodnarchuk M I, Krieg F, Caputo R, Hendon C H, Yang R X, Walsh A and Kovalenko M V 2015 Nanocrystals of cesium lead halide perovskites (CsPbX3, X = Cl, Br and I): novel optoelectronic materials showing bright emission with wide color gamut *Nano Lett.* **15** 3692
[6] Akkerman Q A, Rainò G, Kovalenko M V and Manna L 2018 Genesis, challenges and opportunities for colloidal lead halide perovskite nanocrystals *Nat. Mater.* **17** 394
[7] Buin A, Pietsch P, Xu J, Voznyy O, Ip A H, Comin R and Sargent E H 2014 Materials processing routes to trap-free halide perovskites *Nano Lett.* **14** 6281
[8] Lim J *et al* 2014 Influence of shell thickness on the performance of light-emitting devices based on CdSe/Zn1-xcdxs core/shell heterostructured quantum dots *Adv. Mater.* **26** 8034
[9] Park Y-S, Roh J, Diroll B T, Schaller R D and Klimov V I 2021 Colloidal quantum dot lasers *Nat. Rev. Mater.* **6** 382
[10] Rainò G, Becker M A, Bodnarchuk M I, Mahrt R F, Kovalenko M V and Stöferle T 2018 Superfluorescence from lead halide perovskite quantum dot superlattices *Nature* **563** 671
[11] Fernée M J, Tamarat P and Lounis B 2014 Spectroscopy of single nanocrystals *Chem. Soc. Rev.* **43** 1311
[12] Cundiff S T and Mukamel S 2013 Optical multidimensional coherent spectroscopy *Phys. Today* **66** 44
[13] Fayer M D 2009 Dynamics of liquids, molecules and proteins measured with ultrafast 2D IR vibrational echo chemical exchange spectroscopy *Annu. Rev. Phys. Chem.* **60** 21
[14] Zhuang W, Hayashi T and Mukamel S 2009 Coherent multidimensional vibrational spectroscopy of biomolecules: concepts, simulations and challenges *Angew. Chem., Int. Ed. Engl.* **48** 3750
[15] Dai X, Bristow A D, Karaiskaj D and Cundiff S T 2010 Two-dimensional Fourier-transform spectroscopy of potassium vapor *Phys. Rev.* A **82** 052503
[16] Liang D and Li H 2021 Optical two-dimensional coherent spectroscopy of many-body dipole–dipole interactions and correlations in atomic vapors *J. Chem. Phys.* **154** 214301
[17] Tiwari V, Matutes Y A, Gardiner A T, Jansen T L C, Cogdell R J and Ogilvie J P 2018 Spatially-resolved fluorescence-detected two-dimensional electronic spectroscopy probes varying excitonic structure in photosynthetic bacteria *Nat. Commun.* **9** 4219
[18] Kim J, Jeon J, Yoon T H and Cho M 2020 Two-dimensional electronic spectroscopy of bacteriochlorophyll a with synchronized dual mode-locked lasers *Nat. Commun.* **11** 6029
[19] Fuller F D and Ogilvie J P 2015 Experimental implementations of two-dimensional Fourier transform electronic spectroscopy *Annu. Rev. Phys. Chem.* **66** 667
[20] Nardin G, Autry T M, Moody G, Singh R, Li H and Cundiff S T 2015 Multi-dimensional coherent optical spectroscopy of semiconductor nanostructures: collinear and non-collinear approaches *J. Appl. Phys.* **117** 112804
[21] Cassette E, Dean J C and Scholes G D 2016 Two-dimensional visible spectroscopy for studying colloidal semiconductor nanocrystals *Small* **12** 2234
[22] Moody G and Cundiff S T 2017 Advances in multi-dimensional coherent spectroscopy of semiconductor nanostructures *Adv. Phys.*-X **2** 641
[23] Smallwood C L and Cundiff S T 2018 Multidimensional coherent spectroscopy of semiconductors *Laser Photon. Rev.* **12** 1800171
[24] Bristow A D, Karaiskaj D, Dai X, Zhang T, Carlsson C, Hagen K R, Jimenez R and Cundiff S T 2009 A versatile ultrastable platform for optical multidimensional Fourier-transform spectroscopy *Rev. Sci. Instr.* **80** 073108
[25] Yang L, Zhang T, Bristow A D, Cundiff S T and Mukamel S 2008 Isolating excitonic Raman coherence in semiconductors using two-dimensional correlation spectroscopy *J. Chem. Phys.* **129** 234711
[26] Hamm P and Zanni M 2011 *Concepts and Methods of 2D Infrared Spectroscopy* 1st edn (Cambridge: Cambridge University Press)

[27] Siemens M E, Moody G, Li H, Bristow A D and Cundiff S T 2010 Resonance lineshapes in two-dimensional Fourier transform spectroscopy *Opt. Express* **18** 17699
[28] Mukamel S 1999 *Principles of Nonlinear Optical Spectroscopy* 1st edn (Oxford: Oxford University Press)
[29] Kramer T, Rodríguez M and Zelinskyy Y 2017 Modeling of transient absorption spectra in exciton–charge-transfer systems *J. Phys. Chem.* B **121** 463
[30] Liu A, Almeida D B, Bae W-K, Padilha L A and Cundiff S T 2019 Simultaneous existence of confined and delocalized vibrational modes in colloidal quantum dots *J. Phys. Chem. Lett.* **10** 6144
[31] Liu A, Almeida D B, Bae W K, Padilha L A and Cundiff S T 2019 Non-Markovian exciton-phonon interactions in core-shell colloidal quantum dots at femtosecond timescales *Phys. Rev. Lett.* **123** 057403
[32] Liu A, Nagamine G, Bonato L G, Almeida D B, Zagonel L F, Nogueira A F, Padilha L A and Cundiff S T 2021 Toward engineering intrinsic line widths and line broadening in perovskite nanoplatelets *ACS Nano* **15** 6499
[33] Kuok M H, Lim H S, Ng S C, Liu N N and Wang Z K 2003 Brillouin study of the quantization of acoustic modes in nanospheres *Phys. Rev. Lett.* **90** 255502
[34] Yin Y and Alivisatos A P 2005 Colloidal nanocrystal synthesis and the organic–inorganic interface *Nature* **437** 664
[35] Nasilowski M, Mahler B, Lhuillier E, Ithurria S and Dubertret B 2016 Two-dimensional colloidal nanocrystals *Chem. Rev.* **116** 10934
[36] Utzat H, Shulenberger K E, Achorn O B, Nasilowski M, Sinclair T S and Bawendi M G 2017 Probing linewidths and biexciton quantum yields of single cesium lead halide nanocrystals in solution *Nano Lett.* **17** 6838
[37] Kambhampati P 2021 Nanoparticles, nanocrystals and quantum dots: what are the implications of size in colloidal nanoscale materials? *J. Phys. Chem. Lett.* **12** 4769
[38] Yu B, Zhang C, Chen L, Huang X, Qin Z, Wang X and Xiao M 2021 Exciton linewidth broadening induced by exciton–phonon interactions in CsPbBr3 nanocrystals *J. Chem. Phys.* **154** 214502
[39] Becker M A *et al* 2018 Bright triplet excitons in caesium lead halide perovskites *Nature* **553** 189
[40] Huo C *et al* 2020 Optical spectroscopy of single colloidal CsPbBr3 perovskite nanoplatelets *Nano Lett.* **20** 3673
[41] Liu A 2021 Measuring exciton fine-structure in perovskite nanocrystal ensembles (arXiv:2105.10469 [cond-mat.mes-hall])
[42] Liu A, Almeida D B, Bonato L G, Nagamine G, Zagonel L F, Nogueira A F, Padilha L A and Cundiff S T 2021 Multidimensional coherent spectroscopy reveals triplet state coherences in cesium lead-halide perovskite nanocrystals *Sci. Adv.* **7** eabb3594
[43] Wang L, Williams N E, Malachosky E W, Otto J P, Hayes D, Wood R E, Guyot-Sionnest P and Engel G S 2017 Scalable ligand-mediated transport synthesis of organic–inorganic hybrid perovskite nanocrystals with resolved electronic structure and ultrafast dynamics *ACS Nano* **11** 2689
[44] Accanto N, Masia F, Moreels I, Hens Z, Langbein W and Borri P 2012 Engineering the spin-flip limited exciton dephasing in colloidal CdSe/Cds quantum dots *ACS Nano* **6** 5227
[45] Becker M A *et al* 2018 Long exciton dephasing time and coherent phonon coupling in CsPbBr2Cl perovskite nanocrystals *Nano Lett.* **18** 7546
[46] Liu A and Cundiff S T 2020 Spectroscopic signatures of electron-phonon coupling in silicon-vacancy centers in diamond *Phys. Rev. Mater.* **4** 055202
[47] Ramade J *et al* 2018 Exciton-phonon coupling in a CsPbBr3 single nanocrystal *Appl. Phys. Lett.* **112** 072104
[48] Liu A *et al* 2019 Effect of dimensionality on the optical absorption properties of CsPbi3 perovskite nanocrystals *J. Chem. Phys.* **151** 191103
[49] Zhao W, Qin Z, Zhang C, Wang G, Dai X and Xiao M 2019 Coherent exciton-phonon coupling in perovskite semiconductor nanocrystals studied by two-dimensional electronic spectroscopy *Appl. Phys. Lett.* **115** 243101
[50] Berera R, van Grondelle R and Kennis J T M 2009 Ultrafast transient absorption spectroscopy: principles and application to photosynthetic systems *Photosynth. Res.* **101** 105
[51] Seiler H, Palato S, Sonnichsen C, Baker H, Socie E, Strandell D P and Kambhampati P 2019 Two-dimensional electronic spectroscopy reveals liquid-like lineshape dynamics in CsPbi3 perovskite nanocrystals *Nat. Commun.* **10** 4962
[52] Singh R, Moody G, Siemens M E, Li H and Cundiff S T 2016 Quantifying spectral diffusion by the direct measurement of the correlation function for excitons in semiconductor quantum wells *J. Opt. Soc. Am.* B **33** C137
[53] Liu A, Cundiff S T, Almeida D B and Ulbricht R 2021 Spectral broadening and ultrafast dynamics of a nitrogen-vacancy center ensemble in diamond *Mater. Quantum. Technol.* **1** 025002
[54] Yu B, Chen L, Qu Z, Zhang C, Qin Z, Wang X and Xiao M 2021 Size-dependent hot carrier dynamics in perovskite nanocrystals revealed by two-dimensional electronic spectroscopy *J. Phys. Chem. Lett.* **12** 238
[55] Li X-Q, Nakayama H and Arakawa Y 1999 Phonon bottleneck in quantum dots: Role of lifetime of the confined optical phonons *Phys. Rev.* B **59** 5069
[56] Seibt J and Pullerits T 2013 Beating signals in 2d spectroscopy: electronic or nuclear coherences? application to a quantum dot model system *J. Phys. Chem.* C **117** 18728
[57] Tamarat P, Bodnarchuk M I, Trebbia J-B, Erni R, Kovalenko M V, Even J and Lounis B 2019 The ground exciton state of formamidinium lead bromide perovskite nanocrystals is a singlet dark state *Nat. Mater.* **18** 717
[58] Utzat H *et al* 2019 Coherent single-photon emission from colloidal lead halide perovskite quantum dots *Science* **363** 1068
[59] Hao K *et al* 2016 Direct measurement of exciton valley coherence in monolayer WSe2 *Nat. Phys.* **12** 677
[60] Schaibley J R, Yu H, Clark G, Rivera P, Ross J S, Seyler K L, Yao W and Xu X 2016 Valleytronics in 2D materials *Nat. Rev. Mater.* **1** 16055
[61] Huang X, Chen L, Zhang C, Qin Z, Yu B, Wang X and Xiao M 2020 Inhomogeneous biexciton binding in perovskite semiconductor nanocrystals measured with two-dimensional spectroscopy *J. Phys. Chem. Lett.* **11** 10173
[62] Seiler H, Palato S, Sonnichsen C, Baker H and Kambhampati P 2018 Seeing multiexcitons through sample inhomogeneity: band-edge biexciton structure in CdSe nanocrystals revealed by two-dimensional electronic spectroscopy *Nano Lett.* **18** 2999
[63] Smallwood C L *et al* 2021 Hidden silicon-vacancy centers in diamond *Phys. Rev. Lett.* **126** 213601
[64] Nardin G, Autry T M, Silverman K L and Cundiff S T 2013 Multidimensional coherent photocurrent spectroscopy of a semiconductor nanostructure *Opt. Express* **21** 28617
[65] Cherniukh I *et al* 2021 Perovskite-type superlattices from lead halide perovskite nanocubes *Nature* **593** 535
[66] Mueller S, Lüttig J, Brenneis L, Oron D and Brixner T 2021 Observing multiexciton correlations in colloidal semiconductor quantum dots via multiple-quantum two-dimensional fluorescence spectroscopy *ACS Nano* **15** 4647
[67] Klimov V I 2014 Multicarrier interactions in semiconductor nanocrystals in relation to the phenomena of auger recombination and carrier multiplication *Annu. Rev. Condens. Matter Phys.* **5** 285